Original Article

# Lessons learned from imaging mouse ovarian tumors: the route of probe injection makes a difference

**Myung Shin Han**[1,2], **Ching-Hsuan Tung**[1,2,3]

[1]Molecular Imaging Innovations Institute, Department of Radiology, Weill Cornell Medical College, New York, USA; [2]Department of Translational Imaging, Houston Methodist Research Institute, Houston, TX, USA; [3]Department of Obstetrics and Gynecology, Houston Methodist Hospital, Houston, TX, USA

*Correspondence to:* Ching H. Tung. Weill Cornell Medical College, 413 East 69th Street, Box 290, New York, NY 10021, USA.
Email: cht2018@med.cornell.edu.

**Abstract:** Patients with ovarian cancer often develop small metastatic lesions in their peritoneal cavities. Fluorescent-imaging probes that can highlight these small lesions have significant value for guiding procedures and treatment decisions. In this animal study, we demonstrated that intraperitoneal (IP) delivery of a protease-sensitive fluorescent probe resulted in the labeling of all tumors regardless of their sizes with low background signals in organs. Conversely, intravenous (IV) injections of the probe resulted in high signals in most organs and large tumors (>5 mm) but not in any of the small lesions (<2 mm).

**Keywords:** Optical imaging; fluorescence; intraperitoneal (IP); intravenous (IV)

Submitted Apr 14, 2014. Accepted for publication Apr 16, 2014.
doi: 10.3978/j.issn.2223-4292.2014.04.03
**View this article at:** http://www.amepc.org/qims/article/view/3770/4699

Ovarian cancer is one of the most lethal gynecologic malignancies in the United States, accounting for 6% of cancer-related deaths among women (1). One out of every 68 women will develop ovarian cancer in her lifetime. Early diagnosis of ovarian carcinoma is associated with a high survival rate. However, due to a lack of effective screening methods and the asymptomatic nature of early stages of disease, most patients are diagnosed with advanced, metastatic disease that has spread beyond the ovary. The combination of surgery and chemotherapy effectively reduces tumor burden. After treatment, the disease is typically below the level of detection by physical examination, tumor marker analysis, radiologic evaluation, or second-look laparotomy. Despite achieving clinical remission, a high percentage of patients experience recurrence. Mortality from ovarian cancer is generally due to the development of extensive intra-abdominal metastases.

Standard treatments for ovarian cancer include cytoreductive surgery to remove the bulk of tumor volume and chemotherapy to kill residual tumor cells. Incomplete removal of the primary tumor by surgery or defective killing of residual cancer cells by chemotherapy may be the main reasons for recurrence of ovarian cancer. Sensitive methods to image residual tumor tissues during surgical procedures and to trace recurrent tumors during second-look laparotomies would be clinically beneficial (2). Depending on the stage of cancer and the response of patients, chemotherapeutic agents, such as cisplatin and paclitaxel, may be administered by intravenous (IV) or intraperitoneal (IP) injection (3). The route of infusion does affect the outcome of treatment (4). Clinical studies demonstrate that IP chemotherapy is more effective than conventional IV treatment (5). However, it is not known if IP delivery of an imaging probe provides different information than that of IV delivery in ovarian cancer.

A protease-activated near-infrared fluorescence (NIRF) probe (6) (ProSense®-680) was previously developed and selected for this study. The probe does not emit fluorescence at baseline. However, activation by tumor-associated proteases, such as cathepsin B, L, and S, results in emission of a bright fluorescence signal. Because these cathepsins are commonly upregulated in tumors, this probe has been applied by IV injection to image various tumors, including breast (7), colon (8), pancreatic (9), and ovarian (10).

In this study, we administered the probe by IV or IP injection to a mouse model of peritoneal ovarian cancer. IP injection of the probe resulted in the labeling of all tumors regardless of size. In contrast, IV injection of the probe resulted in the labeling of only the larger tumors. In addition, background fluorescence signals in organs differed depending on the route of injection.

## Materials and methods

### *Cell line and culture*

The SKOV3/GFP-Luc (GFP, green fluorescent protein) human ovarian cancer cell line stably expressing firefly luciferase and GFP was purchased from Cell BioLabs (San Diego, CA, USA). Cells were cultured in McCoy's 5A media supplemented with 2 mM L-glutamine, 10% fetal bovine serum, and 1% penicillin/streptomycin (Gibco BRL, Carlsbad, CA, USA). Cells were maintained at 37 ℃ and 5% $CO_2$ in a humidified incubator.

### *Tumor model and whole-body imaging*

All animal studies were performed in compliance with the approved animal protocols and guidelines of the Institutional Animal Care and Use Committee at Houston Methodist Research Institute. Five-week-old or 6-week-old female BALB/c nude (nu/nu) mice were purchased from Charles River (Wilmington, MA, USA). The animals were maintained in isolation until imaging was initiated.

SKOV3/GFP-Luc cells were collected by trypsinization, centrifuged at 1,000 rpm for 5 min at 4 ℃, washed twice with PBS, and re-suspended in normal saline at a density of $5\times10^7$ cells per mL prior to IP injection (200 µL). One or two weeks after injection, SKOV3/GFP-Luc tumor growth was monitored by bioluminescence imaging with a small animal optical-imaging system (IVIS-200, PerkinElmer, Boston, MA, USA) immediately after injecting D-Luciferin (2 mg in 150 µL of PBS, Regis Technologies, Morton Grove, IL, USA). Mice with intense bioluminescence signals were divided into two groups of four mice each. Due to IP injection of cancer cells, tumors grew randomly in the peritoneal cavity and on the surfaces of organs. Each mouse received either IV or IP injection of the ProSense®-680 probe (2 nmole in 200 µL of PBS, PerkinElmer). All mice were sacrificed by inhalation of $CO_2$ gas and cervical dislocation one day after the probe was injected. The abdomen of each mouse was opened and imaged using a GFP-filter set or a Cy5.5-filter set on a Maestro™ imaging system (PerkinElmer).

### *Fluorescence imaging and signal analysis of excised organs*

After whole-body imaging, organs and tissues, including the spleen, liver, intestine, stomach, kidney, muscle, and large solid tumors (>5 mm) were collected and placed on glass slides for fluorescence imaging with Maestro (PerkinElmer). Regions of interest (ROI, 450 pixels for each location) were examined to measure the average fluorescence efficiency with the manufacturer's software (Version 3.0.1).

### *Histological validation with anti-CD34+/+ staining*

Dissected snap-frozen tissues were embedded in Optimal Cutting Temperature compound (Sakura Finetek, Torrance, CA, USA) and serially sectioned into 15-µm and 6-µm sections. Thick (15-µm) sections were used for fluorescent imaging after covering slides with coverslips in the presence of mounting media. Thin (6-µm) sections were used for histological staining, including CD34 staining for vascular endothelial cells in tumor tissues and H&E staining for general morphology. Slides of frozen sections were thawed for 10-20 min at room temperature and rehydrated in washing buffer for 10 min for CD34 staining. Excess washing buffer was drained, and slides were incubated with anti-CD34 antibody (GeneTex, Irvine, CA, USA) for 30 min at room temperature. The slides were then incubated with horseradish peroxidase (HRP)—labeled secondary antibody (Thermo, Fremont, CA, USA) for 30 min at room temperature. Slides were incubated with DAB Plus substrate (Invitrogen, Camarillo, CA, USA) for 15 min, counterstained with hematoxylin solution, and then covered. Slides were imaged with a fluorescence microscope (I×81, Olympus, Tokyo, Japan). Fluorescence images were captured with a spectrally resolved filters of Cy5.5 (excitation: 650 nm, emission: 710 nm) and GFP (excitation: 470 nm and emission: 525 nm). Slides that were stained for CD34 and H&E were captured with bright light at 4× and 10× magnifications.

## Results

The animal model of peritoneal ovarian cancer was prepared by inoculating SKOV3/GFP-Luc ovarian cancer cells into nude mice by IP injection. Tumor cells randomly engrafted onto the surfaces of tissues and organs, imitating the clinical

 

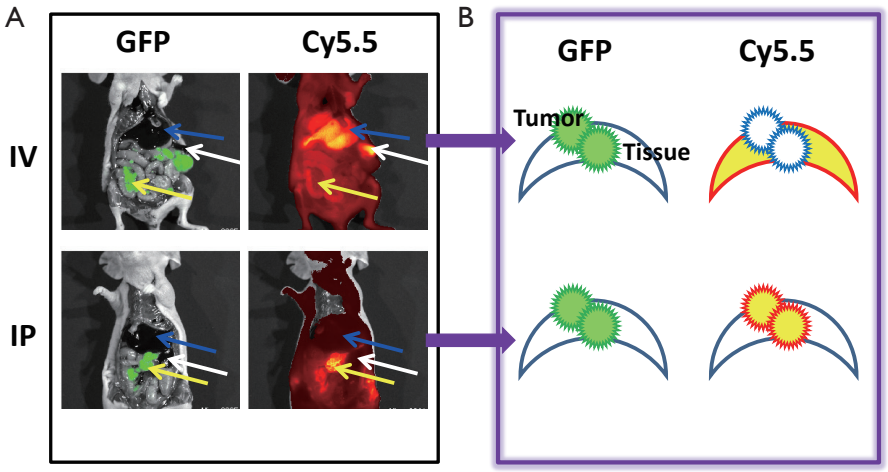


**Figure 1** Fluorescence images of ovarian tumors with ProSense (2 nmoles) delivered through IV or IP injection 24 h before imaging. (A) GFP signal indicated the location of the SKOV3 tumor, and Cy5.5 images showed the protease-activated ProSense signal. IV injection of the probe resulted in high Cy5.5 signals in the liver (blue arrow) and spleen (white arrow) but not in small tumors (yellow arrow). In contrast, IP injection of the probe resulted in high Cy5.5 signals in tumors and low signals in the liver and spleen; (B) Schematic drawing of the fluorescence contrast between tumors and organs according to the route through which the probe is administered. GFP, green fluorescent protein; IV, intravenous; IP, intraperitoneal.

situation of ovarian cancer. Tumor growth was followed by bioluminescence imaging of the engineered luciferase gene. About two weeks after inoculation, ProSense-680 (2 nmoles) was delivered by IV injection through the tail vein or IP injection directly into the abdomen. Animals were sacrificed one day after the probe was injected. Gross images were obtained in white light, or in a GFP or Cy5.5 channel with corresponding filter sets (*Figure 1*). Tumor lesions were located clearly on the GFP images, because the tumor cells stably expressed GFP. The sensitivity and selectivity of ProSense were validated by overlaying the Cy5.5 images with the GFP images. Gross examinations showed that the IV-injected probe resulted in strong signals in the liver and spleen but failed to image small tumors (<2 mm). In contrast, the IP-injected probe highlighted small tumors with low background signals in various organs.

Tumors and organs were collected and imaged at the macroscopic scale. Similar to what was observed by whole-body imaging, high background fluorescent signals were observed in several organs, especially the liver, spleen, kidney, stomach, and guts, when the probe was administered by IV injection (*Figure 2*). Large tumors (>5 mm) were also positive for Cy5.5 fluorescence, whereas the small tumors engrafted on the surfaces of organs were mostly negative for Cy5.5 fluorescence. Conversely, IP injection of the probe resulted in bright fluorescence in large and small tumors, including those that were <1 mm in size. In addition, the background signals were very low in most organs except for the kidneys.

ROI analysis confirmed the imaging results for the IP- versus IV-injected probe (*Figure 3*). In comparison to muscle in which the Cy5.5 background signal was low, all tumors exhibited high contrast (>5-fold) regardless of the injection route. However, comparisons of the signal intensities of large tumors with those of organs showed that the IV-injected probe failed to distinguish tumors from organs due to the high background Cy5.5 signals in organs. Furthermore, the IV-injected probe failed to visualize all of the small tumors regardless of location. In contrast, the IP-injected probe offered significant contrast in small and large tumors located on the surfaces of the intestine (>2.5-fold), spleen (>4.5-fold), liver (>1.5-fold), and stomach (~1.3-fold) but not on the kidney (<0.6-fold).

Collected tissues from small tumors were sliced and examined histologically. A close correlation was observed between the GFP tumor signal and the Cy5.5 ProSense signal in the IP-injected group (*Figure 4*). As previously observed, the Cy5.5 probe signal was not detected in small tumors if the probe was applied by IV injection. The non-homogeneous probe distribution may contribute to the differences among images. Tumor vasculature was examined by staining for CD34, a sensitive and well-studied marker of the vascular endothelium. Immunohistochemical staining

 

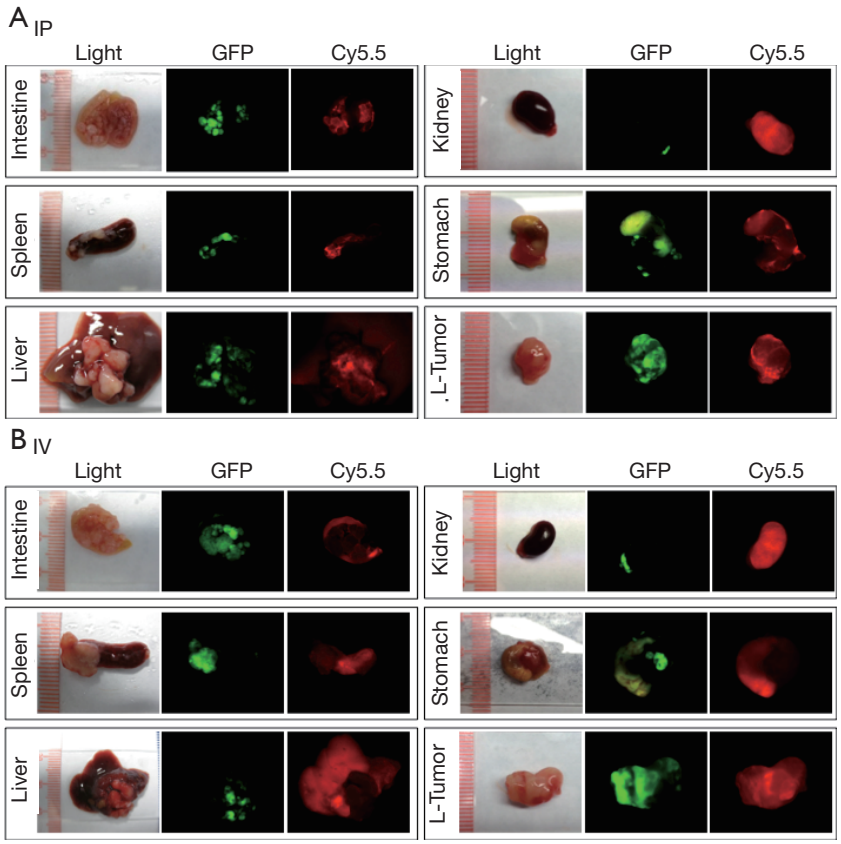


**Figure 2** *Ex vivo* comparison of ProSense-contrasted ovarian cancer in individual organs. (A) IP delivery; the tumor GFP signal correlated well with the ProSense fluorescence signals; (B) IV delivery; the Cy5.5-fluorescent background signals in organs were higher than those of small tumors. L-Tumor: large tumor (>5 mm). IP, intraperitoneal; IV, intravenous; GFP, green fluorescent protein.

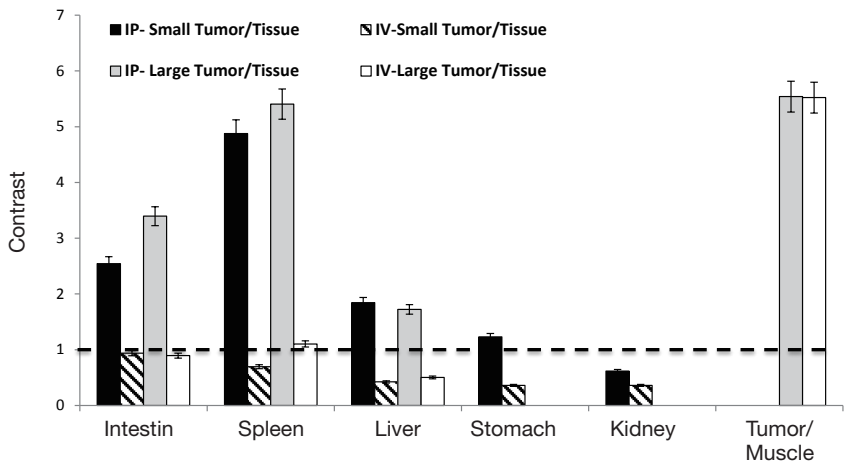


**Figure 3** Quantification of the NIRF signal with a tumor to organ ratio. The contrast (y-axis) was calculated by dividing the fluorescence intensity of tumors to it of specific tissues. High background organ signals resulted in poor contrasts (≤1). NIRF, protease-activated near-infrared fluorescence; IP, intraperitoneal; IV, intravenous.

 

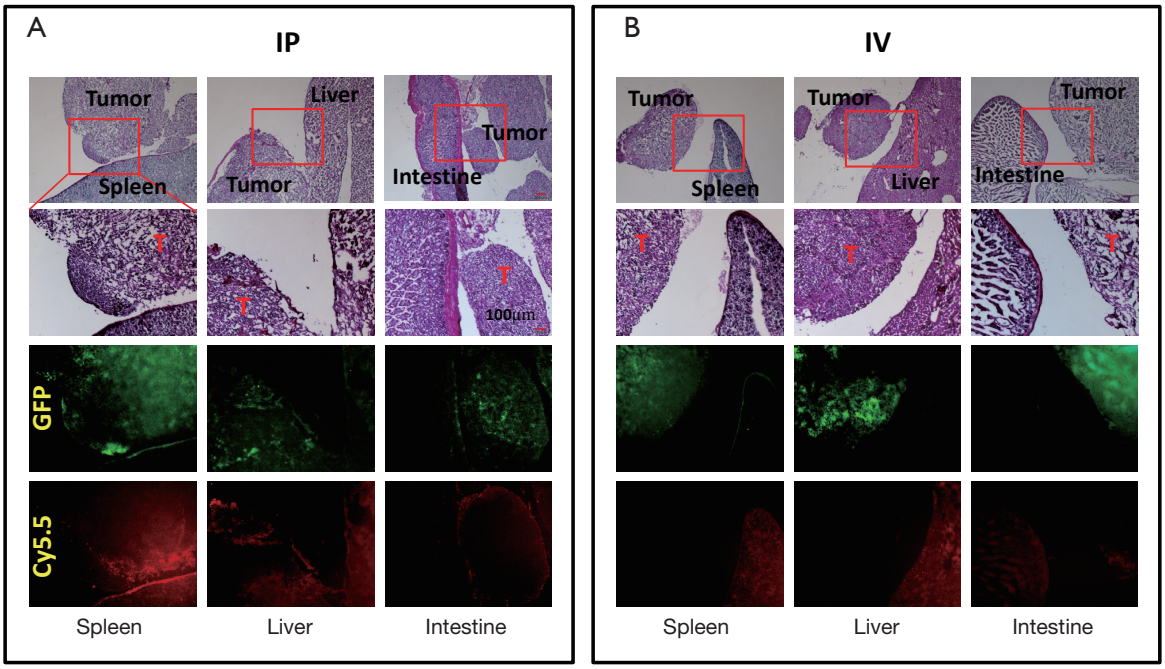


**Figure 4** Histological correlations between tumor signals (GFP) and Cy5.5 signals. (A) IP delivery; (B) IV delivery. T, tumor; GFP, green fluorescent protein; IP, intraperitoneal; IV, intravenous.

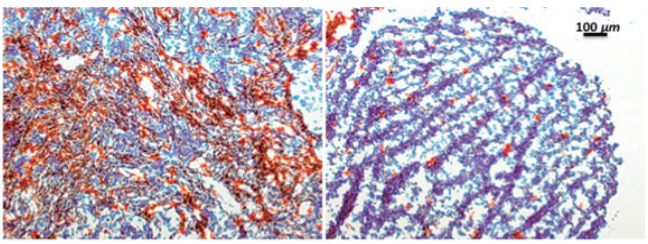


**Figure 5** CD34 staining of vascular endothelium in large tumor and small tumor; 10× magnification.

showed a dense network of microvessels in large tumors, whereas only a few microvessels were scattered within small tumors (*Figure 5*). These differences in tumor vasculature may explain the poor ability of the IV-injected probe to detect small tumors.

## Discussion

Significant differences in vascular density were observed by CD34 staining in tumors of different sizes. The vascular network is a critical component of tumor growth, because all nutrients and oxygen are transported through blood vessels. In the absence of sufficient blood supply, solid tumors cannot grow beyond 1-2 mm in size (11). Vascularity also affects probe delivery to tumors. The IV-injected probe circulates in blood vessels and extravasates into interstitial spaces. Delivery of the IV-injected probe is efficient in big tumors. Effective delivery of the probe results in high signals in organs and large tumors. Conversely, small ovarian epithelial tumors, which have poorly differentiated vasculature, must directly absorb nutrients through the epithelial membrane. The IP-injected probe efficiently enters small tumors by direct absorption and is activated by locally enriched tumor-associated proteases. However, the epithelial membranes of major intra-abdominal organs might not absorb the probe as efficiently as that of the neoplastic lesions. Thus, the background signals in organs are much lower in the IP-injected group. The kidney was an exception, because it showed a high Cy5.5 signal regardless of the route through which the probe was administered. Since background signal greatly dominates the image contrast ratio (12), a high background signal in kidney results in poor contrast.

In most cases of ovarian cancer, patients have small metastatic lesions at the time of diagnosis. Complete removal of neoplastic lesions may reduce the chance of recurrence, but the identification and removal of all small

 

lesions is a challenge. In some high-risk patients, second-look laparotomy, which uses white-light imaging to survey the peritoneal cavity for small micro-metastases, is performed to evaluate the efficacy of the initial treatment or to identify recurrence. Several fluorescence-imaging agents that were recently developed to label lesions may be helpful for guiding these procedures (10,13,14). However, because most residual or recurrent tumors are small, it is possible that IV delivery will not adequately allow imaging probes to reach small lesions, resulting in false-negative results. Based on our observations, IP administration of imaging probes, such as ProSense, is a more effective approach for detecting small neoplastic lesions.

Small neoplastic tumors directly absorb sufficient quantities of nutrients through their epithelial membranes. Direct absorption can internalize a broad spectrum of molecules, including the polymer-based ProSense, which was used in this study. Various cathepsins are overexpressed during all stages of ovarian cancer (15,16). Thus, activation of ProSense occurs within these lesions. The fluorescence-imaging protocol described here could be extremely valuable for directing treatment. However, our results also highlight the potential inability of IV-infused chemotherapeutic agents to reach tumors, resulting in residual cancer cells surviving after chemotherapy. Although those tumors are small and in "complete remission", recurrence may be anticipated. Such inefficient delivery of chemotherapeutic agents may also contribute to serious drug resistance issue which is often seen in patients with advanced-stage ovarian cancer (17).

## Conclusions

In this report, an orthotopic model of ovarian cancer was used to study the effects of the route of administration of an imaging probe on tumor contrast. The IV-injected probe was distributed through the vasculature to all organs and large tumors. Strong fluorescence signals were detected in areas with high local protease activity, such as the liver, kidney, spleen, intestine, and tumors. However, the IV-injected probe did not highlight small neoplastic lesions, possibly due to an underdeveloped vascular network. Conversely, the IP-injected probe detected large and small tumors, probably because it was absorbed directly through the epithelial membranes. The IP-injected group also showed lower background signals in various organs. Our observations indicate that IP delivery of an imaging probe is more efficient for detecting small ovarian cancer lesions.

## Acknowledgements

*Funding:* This research was supported in part by NIH CA135312 and the Oshman Foundation.
*Disclosure:* The authors declare no conflict of interest.

## References

1. Siegel R, Naishadham D, Jemal A. Cancer statistics, 2012. CA Cancer J Clin 2012;62:10-29.
2. Tung CH. Colorful lighting in the operating room. Quant Imaging Med Surg 2013;3:186-8.
3. Armstrong DK, Bundy B, Wenzel L, et al. Intraperitoneal cisplatin and paclitaxel in ovarian cancer. N Engl J Med 2006;354:34-43.
4. Walker JL. Intraperitoneal chemotherapy for ovarian cancer: 2009 goals. Gynecol Oncol 2009;112:439-40.
5. Schmid BC, Oehler MK. New perspectives in ovarian cancer treatment. Maturitas 2014;77:128-36.
6. Weissleder R, Tung CH, Mahmood U, et al. In vivo imaging of tumors with protease-activated near-infrared fluorescent probes. Nat Biotechnol 1999;17:375-8.
7. Bremer C, Tung CH, Bogdanov A Jr, et al. Imaging of differential protease expression in breast cancers for detection of aggressive tumor phenotypes. Radiology 2002;222:814-8.
8. Marten K, Bremer C, Khazaie K, et al. Detection of dysplastic intestinal adenomas using enzyme-sensing molecular beacons in mice. Gastroenterology 2002;122:406-14.
9. Eser S, Messer M, Eser P, et al. In vivo diagnosis of murine pancreatic intraepithelial neoplasia and early-stage pancreatic cancer by molecular imaging. Proc Natl Acad Sci USA 2011;108:9945-50.
10. Sheth RA, Upadhyay R, Stangenberg L, et al. Improved detection of ovarian cancer metastases by intraoperative quantitative fluorescence protease imaging in a pre-clinical model. Gynecol Oncol 2009;112:616-22.
11. Folkman J. Angiogenesis in cancer, vascular, rheumatoid and other disease. Nat Med 1995;1:27-31.
12. Frangioni JV. The problem is background, not signal. Mol Imaging 2009;8:303-4.
13. van Dam GM, Themelis G, Crane LM, et al. Intraoperative tumor-specific fluorescence imaging in ovarian cancer by folate receptor-α targeting: first in-human results. Nat Med 2011;17:1315-9.
14. Urano Y, Sakabe M, Kosaka N, et al. Rapid cancer detection by topically spraying a γ-glutamyltranspeptidase-

 

activated fluorescent probe. Sci Transl Med 2011;3:110ra119.
15. Downs LS Jr, Lima PH, Bliss RL, et al. Cathepsins B and D activity and activity ratios in normal ovaries, benign ovarian neoplasms, and epithelial ovarian cancer. J Soc Gynecol Investig 2005;12:539-44.
16. Nishikawa H, Ozaki Y, Nakanishi T, et al. The role of cathepsin B and cystatin C in the mechanisms of invasion by ovarian cancer. Gynecol Oncol 2004;92:881-6.
17. Cooke SL, Brenton JD. Evolution of platinum resistance in high-grade serous ovarian cancer. Lancet Oncol 2011;12:1169-74.

**Cite this article as:** Han MS, Tung CH. Lessons learned from imaging mouse ovarian tumors: the route of probe injection makes a difference. Quant Imaging Med Surg 2014;4(3):156-162. doi: 10.3978/j.issn.2223-4292.2014.04.03

 